EXHIBIT S

TO DECLARATION OF S. MERRILL WEISS IN SUPPORT OF PLAINTIFF ACACIA MEDIA TECHNOLOGIES CORPORATION'S MEMORANDUM OF POINTS AND AUTHORITIES IN OPPOSITION TO ROUND 3 DEFENDANTS' MOTION FOR SUMMARY JUDGMENT OF INVALIDITY UNDER 35 U.S.C. § 112 OF THE '992, '863, AND '702 PATENTS; AND SATELLITE DEFENDANTS' MOTION FOR SUMMARY JUDGMENT OF INVALIDITY OF THE '992, '863, AND '720 PATENTS

A NEW AUDIO BIT RATE REDUCTION SYSTEM FOR THE CD-I FORMAT

2375 (C-4)

Masayuki Nishiguchi
Kenzo Akagiri
Tadao Suzuki
Sony Corporation
Information Systems Research Center
Tokyo, Japan

Presented at the 81st Convention 1986 November 12-16 Los Angeles, California

AN AUDIO ENGINEERING SOCIETY PREPRINT

A NEW AUDIO BIT RATE REDUCTION SYSTEM FOR THE CD-I FORMAT

Masayuki Nishiguchi, Kenzo Akagiri, Tadao Suzuki
Information Systems Research Center, Sony Corporation
1-7-4, Konan, Minato-ku, Tokyo, Japan

ABSTRACT

This paper describes a newly developed audio bit rate reduction system for the CD-I (Compact Disc Interactive) format. The bit rate reduction system is based on the fact that the spectrum and amplitude distribution of audio signals tends to be concentrated in a certain region. We have developed an algorithm of the bit rate reduction system and built both an encoder using DSPs and a dedicated decoder LSI.

The present system allows us to record and reproduce audio signals of three different bit rates to match specific applications:

Level A: Audio signals whose quality is almost the same as that obtainable with Compact Discs, using 309 Kbits/second per channel.

Level B: Audio signals of slightly lower quality than Level A, but still suitable for high-quality music, using 159 Kbits/second per channel.

Level C: Audio signals for recording and reproduction of high-quality speech, using 80 Kbits/second per channel.

1. INTRODUCTION

In 1985 the CD-ROM system was developed in order to utilize Compact Discs as computer data storage media. The CD-I format, formulated by Sony and Philips, is an application of the CD-ROM and allows us to integrate still-picture data, computer software, and audio data on a single Compact Disc. For instance, a single CD-I disc can memorize 60 minutes of high-fidelity stereo music (Level A) and 3600 natural images, and we can access any image or any music in an interactive mode. In order to realize the CD-I format, audio data have to be compressed without perceptible degraduation or reduction of the error-concealment capability. In addition, it is desirable that the structure of the decoder be simple.

2. CD-I SYSTEM

2.1. Data structure of CD-I audio sector

Figure 1 shows the structure of the CD-I audio sector. The basic sector of the CD-I format consists of 2352 bytes, including a sync pattern, a header, a subheader and 2324 bytes of user data. One audio sector contains 18 sound groups (SG) in its user area. One sound group consists of 4 or 8 sound blocks. The number of sound blocks in one sound group depends on the word length of the residual data. One sound block comprises 28 samples.
Bit compression and expansion is carried out with this sound block regarded as one unit. Sound parameters (range and filter) are generated every sound block.

2.2. Construction of CD-I system hardware

In Figure 2, the overall block diagram of the prototype CD-I encoder-decoder system, which includes the bit rate reduction system, is shown. Note that the SRC (Sampling Rate Converter), the block encoder and the BRR (Bit Rate Reduction) encoder use DSPs.

2.2.1. Encoder system

Audio data, whose sampling frequency is 44.1 KHz and word length is 16 bits/sample, are inputted to the SRC from a CDP (Compact Disc Player) or PCM processor via a digital audio interface. The sampling rate is converted from 44.1 KHz to 37.8 KHz or 18.9 KHz with the SRC.

The word length is compressed to 8 or 4 bits/sample with the BRR encoder, then residual data and additional information (range and filter) are inputted to the block encoder. A subheader is added to these data and the result is formed by the block encoder into a block that consists of 2,336 bytes. Block-structured data are multiplexed with picture data and computer data. A sync and header are added to these data, which are then scrambled.
After this stage, the same processing (ECC,EFM) as that of a current CD mastering system is executed.

2.2.2. Decoder system

Data read from the disc are inputted to a descrambler and sync-detector via an EFM demodulator and ECC decoder.
Sound blocks are chosen and headers are removed by the data selector. In the sound decorder, first, interpolation is executed by the error compensator when the input has an error flag.
Inputted data are then block-decoded and expanded to linear 16-bit data by the BRR decoder.

The next stage has three steps: D/A conversion, low pass filtering, and de-emphasis. The D/A conversion speed and the cut-off frequency of the LPF must be changed with the sampling rate, or an over-sampling digital filter can be used.

3. BIT RATE REDUCTION SYSTEM

3.1. Overall view of the bit rate reduction system

The principal feature of this system is that it provides multiple prediction filters in order to respond effectively to fluctuations in the frequency distribution of the signal. In order to obtain a high instantaneous S/N, some combination of a 1st-order and two kinds of 2nd-order differential PCM modes are used for signals in the low and middle frequencies and the straight PCM mode is used for high-frequency signals.

This system also employs near-instantaneous companding to expand the dynamic range. A noise-shaping filter is incorporated in the quantization stage, and its frequency response is varied to minimize the energy of the output noise. By separating the noise shaping filter from the prediction filter, the selection of the optimum filter becomes easier.

3.2. Algorithm of the BRR system

Figure 3 shows the block diagram of the BRR system.
Firstly, we express the input signal, prediction error, quantization error, encoder output, decoder input and decoder output as $x(n)$, $d(n)$, $e(n)$, $\hat{d}(n)$, $\hat{d}'(n)$ and $\hat{x}'(n)$, respectively. Secondly, we define the z-transform of each signal as $X(z)$, $D(z)$, $E(z)$, $\hat{D}(z)$, $\hat{D}'(z)$ and $\hat{X}'(z)$, respectively.
Then we can express the encoder response as

$$\hat{D}(z)=G\cdot X(z)\cdot\{1-P(z)\}+E(z)\cdot\{1-R(z)\}. \qquad --(1)$$

(See Appendix I for the derivation of Eq.(1).)

And the decoder response is written as

$$X'(z)=\frac{G^{-1}\cdot\hat{D}'(z)}{1-P(z)} \quad . \qquad --(2)$$

(See Appendix II for the derivation of this equation.)

Now, assuming that there is no error in the signal recorded media, we can write $\hat{D}'(z)=\hat{D}(z)$. From Eq.(1) and (2), using the encoder input X(z) the decoder output is written as follows:

$$\hat{X}'(z)=X(z)+G^{-1}\cdot E(z)\,\frac{1-R(z)}{1-P(z)} \qquad --(3)$$

where

$$P(z)=\sum_{k=1}^{p}\alpha k\cdot z^{-k}$$

$$R(z)=\sum_{k=1}^{q}\beta k\cdot z^{-k}$$

Eq.(3) shows the encoder-decoder performance characteristics of the BRR system. It shows that the quantization error E(z) is reduced by the extent of the noise-reduction effect G^{-1}. The distribution of the noise spectrum that appears at the decoder output is

$$N(z)=E(z)\cdot\frac{1-R(z)}{1-P(z)}\ ,$$

We ordinarily set R(z)=P(z) to whiten the noise.

G can be regarded as the normalization factor for the peak prediction error (over 28 residual words) from the chosen prediction filter. G has its own frequency response. To simplify the analysis, we divide G into two parts:

$$G=Gp\cdot Gf,$$

where Gp is the prediction gain in the prediction filter. Gp represents the gain in the instantaneous signal-to-noise ratio (SNR) that is due to the differential scheme. Gf represents the gain in the dynamic range that is due to block floating. Then, Gp is not dependent upon the amplitude of input signals but is dependent upon the frequency of input signals. On the other hand, Gf is not dependent upon the frequency of input signals but is dependent upon the amplitude of input signals.

Now, Gp can be written as

$$Gp=\frac{X(z)}{D(z)}=\frac{1}{1-P(z)}\ ,$$

which represents the frequency response of the gain in SNR, which is the inverse function of the prediction filter 1-P(z). So, it is necessary to change the frequency characteristics of the prediction filter 1-P(z) according to the frequency distribution of the input signals. Next, we will show how the encoder chooses the optimum filter.

3.3. Selection of the optimum filter

Several different strategies of selecting filters are possible in the CD-I format. The simplest is as follows.

Figure 4 shows the detailed configuration of the prediction filters. In this figure, we designate the four prediction filters as PF1, PF2, PF3 and PF4. Basically the encoder chooses which predictor is most suitable in the following manner:

1. The predictor adaptation section in Fig.4 compares the peak value of the prediction errors (over 28 words) from each prediction filter 1-P(z) to find the minimum peak. The predictor adaptation section then selects the filter which generates the minimum peak.

2. The group of prediction errors chosen is gain controlled (normalized by its maximum value) and noise shaping is executed at the same time.

As a result of the above strategy, PF2, PF3 and PF4 in Fig.4 are used for signals in the low and middle frequencies and PF1 is used for high-frequency signals, in order to obtain a high instantaneous S/N.

Suppose that the system has only two prediction filters, namely, the straight PCM mode and the 1st order differential PCM mode. In this case, the switching frequency (at which a prediction filter is switched) will be at fs/6. Figure 5 shows this situation.

In an ordinary DPCM (fixed prediction) system, when the signal has predominantly high-frequency components, the signal becomes susceptible to code errors because :

1. The prediction filter has a negative prediction gain in the high frequencies.

2. Accurate interpolation cannot be carried out by averaging or 0 order hold.

In this event, this system operates in the straight PCM mode so it can reduce the effect of code errors.

3.4. Detailed configuration of the BRR system

This system provides three bit rates for the CD-I format, and data encoded using any bit rate can be decoded by a single decoder. In the following sections, we explain how the parameters employed in both the decoder and the encoder would change according to level A, B, and C. Table I shows the parameters for each level.

3.4.1. Level A

We can obtain the highest quality audio sound with this level. As we have seen in Fig.4, the system has four prediction filters. This level uses only two filters. Either the straight PCM mode or the 1st-order differential PCM mode is selected.
The transfer functions of prediction filters are as follows.

$$H(z)=1 \quad \text{----- Straight PCM mode} \quad --(4)$$

$$H(z)=1-0.9375\cdot z^{-1} \quad \text{----- 1st-order differential PCM mode,} \quad --(5)$$

where $H(z)=1-P(z)$.

3.4.2. Level B

At this level, we use a bit rate half as high as Level A. By using this level, we can obtain high-fidelity audio sound from most high quality sources. This level uses three filters: the straight PCM mode, the 1st-order differential PCM mode, or the 2nd-order differential PCM-1 mode is selected. The transfer functions of the first two filters are the same as in Level A, and in addition, the 2nd order differential PCM-1 mode:

$$H(z)=1-1.796875\cdot z^{-1}+0.8125\cdot z^{-2} \quad --(6)$$

is used.

3.4.3. Level C

Using this level, we can obtain high-quality voice sound. At this level, a monaural audio program 16 hours long can be recorded on a single Compact Disc. All four filters are used for this level. The transfer functions of the first three filters are the same as in Level B. The transfer function of the 2nd-order differential PCM-2 mode, used only by this level, is

$$H(z)=1-1.53125\cdot z^{-1}+0.859375\cdot z^{-2}. \quad --(7)$$

The noise shaping filter and the prediction filter in the decoder have the same coefficients as the prediction filter in the encoder through all levels.

The above are the coding formats of the BRR system.

Now, we will report the frequency responses of transfer functions $1-P(z)$.

Figure 6 shows the frequency response of the 1st-order differential PCM mode as expressed in Eq.(5) when fs=37.8 KHz. Figure 7 shows the frequency response of the 2nd-order differential PCM-1 mode as expressed in Eq.(6) when fs=37.8 KHz. Figure 8 shows the frequency response of the 2nd-order differential PCM-2 mode as expressed in Eq.(7) when fs=18.9 KHz.

4. EXPERIMENTAL RESULTS

4.1 Encoder-decoder performance characteristics

Employing the above parameters, we measured the encoder-decoder performance characteristics. Figure 9 shows the measurement block diagram. Figure 10 shows the signal-to-noise ratio at each level versus the input level at 1 KHz. At Level C, we measured the SNR with emphasis OFF because at this level this system should be used with emphasis OFF. The dynamic range of all three levels is over 98 dB. The bandwidth of Level A and B is 17 KHz, and that of Level C is 8.5 KHz. The frequency response of the maximum output level is the same as de-emphasis(15-50 μS) when we use the system with emphasis ON; otherwise it is flat at all frequencies.

4.2. Error concealment capability

We carried out hearing tests using many kinds of music sources to test the error concealment capability of the bit rate reduction system.

In order to simulate the occurance of code errors, we generated 8-bit pseudo-random numbers using the following three polynomials.

$$X^8+X^4+X^3+X^2+1 \quad \text{--(10)}$$

$$X^8+X^6+X^5+X^3+1 \quad \text{--(11)}$$

$$X^8+X^6+X^5+X^2+1 \quad \text{--(12)}$$

If the generated 8-bit number was no greater than the threshold, the signal symbol was declared erroneous. Any error rate can be obtained by setting the appropriate threshold.

We assumed that there are only three successive erroneous sectors per second, of which 3% of the symbols are in error. Figure 11 shows the distribution of errors along the time axis. 3% is the maximum error rate actually measured on Compact Discs with artificial scratches on them. In normal operating conditions, an error of three sectors with 3% erroneous symbols occurs at most once an hour. (A "sector" means 2,352 bytes in the CD-I format.)

We obtain following results.

Level A --- There was no audible noise at all.
Level B --- There was a slight noise, but it was less audible than the scratch noise of conventional audio discs.
Level C --- The same as Level B.

From the above experiments, we conclude that the error concealment capability of the BRR system is more than sufficient for practical use.

5. DECODER LSI

We designed a dedicated decoder LSI which uses about 5000 gates. Figure 12 shows the block diagram of the LSI. The LSI has three main parts: the error compensator, the block decoder and the BRR decoder. The LSI generates linear 16-bit data which can be inputted directly to a D/A converter from the block structured data as in Fig.1. The LSI is used together with an external 64K DRAM, and can decode stereo signals at any level.

6. CONCLUSION

The new audio bit rate reduction system offers advantages in its good sound quality, good error-concealment capability and the simple structure of the decoder which has already been realized in an LSI designed to meet practical applications.

7. ACKNOWLEDGEMENTS

The authors would like to thank Mr. H. Yoshida, Director of the Sony Information Systems Research Center, Mr. T. Waku, Director of the Fourth Research Group of the Research Center, Mr. O. Hamada, Mr. Y. Katsumata, Assistant Managers of the Fourth Group of the Research Center, Mr. T. Uematsu, Assistant Manager of the Semicoductor Division, Mr. S. Masuda, an engineer in the Semiconductor Division, and all members of the CD-I project.

8. REFERENCES

[1] M. Nishiguchi and K. Akagiri,"Audio Bit Rate Reduction System," Proc. Spring Meet. Acoust. Soc. Jpn., 313-314(1984)

[2] L. R. Rabiner and R. W. Schafer, Digital Processing of Speech Signals, Prentice-Hall, 1978

[3] A. V. Oppenheim and R. W. Schafer, Digital Signal Processing, Prentice-Hall, 1975

Appendix I

First let us obtain the output from the encoder expressed as a function of z. We express the input signal as x(n) and its predicted value as $\tilde{x}(n)$. Then the difference signal d(n) can be written as

$$d(n)=x(n)-\tilde{x}(n). \qquad --(13)$$

The predicted value $\tilde{x}(n)$ can be expressed as a linear combination of past input values x(n-k) as

$$\tilde{x}(n)=\sum_{k=1}^{p}\alpha k\cdot x(n-k). \qquad --(14)$$

Note that the predicted value is thus the output of an FIR (Finite Impulse Response) filter whose system function is

$$P(z)=\sum_{k=1}^{p}\alpha k\cdot z^{-k}. \qquad --(15)$$

From Eq.(13) and (14), we can obtain

$$d(n)=x(n)-\sum_{k=1}^{p}\alpha k\cdot x(n-k), \qquad --(16)$$

which is the difference between input sample x(n) and the predicted value $\tilde{x}(n)$. We call this difference signal d(n) the prediction error.

Then prediction errors are gain controlled to be normalized by their maximum value, and noise shaping is executed at the same time. Next, we show this processing.

We define d'(n) as

$$d'(n)=d(n)-\tilde{e}(n), \qquad --(17)$$

where $\tilde{e}(n)$ is the predicted value of the quantization error. We also write d"(n) as

$$d"(n)=G\cdot d'(n), \qquad --(18)$$

where G is the gain of the shifter in Fig.3.
The processing of the quantization of d"(n) can be represented as

$$\hat{d}(n)=d"(n)+e(n), \qquad --(19)$$

where e(n) is the quantization error.
The $\tilde{e}(n)$ in the Eq.(17) can explicitly be written as

$$\tilde{e}(n)=\sum_{k=1}^{R}\beta k\cdot e(n-k)\cdot G^{-1}, \qquad --(20)$$

whose form is the same as $\tilde{x}(n)$ in Eq.(14). Namely, predicted value $\tilde{e}(n)$ is also a linear combination of past quantization errors e(n-k).

The system function of the FIR filter for noise shaping is

$$R(z)=\sum_{k=1}^{R}\beta k\cdot z^{-k}\ . \qquad --(21)$$

From Eq.(17),(18),(19) and (20), we obtain

$$\begin{aligned}\hat{d}(n)&=G\cdot\{d(n)-\tilde{e}(n)\}+e(n)\\&=G\cdot d(n)+e(n)-\sum_{k=1}^{R}\beta k\cdot e(n-k)\ .\end{aligned} \qquad --(22)$$

Using Eq.(16) we rewrite the above expression as

$$\hat{d}(n)=G\cdot\{x(n)-\sum_{k=1}^{P}\alpha k\cdot x(n-k)\}+e(n)-\sum_{k=1}^{R}\beta k\cdot e(n-k)\ . \qquad --(23)$$

Now we define the z-transform of $x(n)$, $e(n)$ and $\hat{d}(n)$ as $X(z)$, $E(z)$, $\hat{D}(z)$. Then Eq.(23) becomes

$$\begin{aligned}\hat{D}(z)&=G\cdot X(z)\cdot(1-\sum_{k=1}^{P}\alpha k\cdot z^{-k})+E(z)\cdot(1-\sum_{k=1}^{R}\beta k\cdot z^{-k})\\&=G\cdot X(z)\cdot\{1-P(z)\}+E(z)\cdot\{1-R(z)\}.\end{aligned}$$

Appendix II

We derive the decoder response in the following manner. Referring to Fig.3 again,

$$\hat{d}''(n)=\hat{d}'(n)\cdot G^{-1} \qquad --(24)$$

and

$$\hat{x}'(n)=\hat{d}''(n)+\tilde{x}'(n)\ . \qquad --(25)$$

From the above two equations, decoder output $\hat{x}'(n)$ can be written as

$$\hat{x}'(n)=\hat{d}'(n)\cdot G^{-1}+\sum_{k=1}^{P}\alpha k\cdot\hat{x}'(n-k)\ . \qquad --(26)$$

Similarly, we denote the z-transform of $\hat{x}'(n)$ and $\hat{d}'(n)$ as $\hat{X}'(z)$, $\hat{D}'(z)$. Then $\hat{X}'(z)$ can be written from Eq.(26) as

$$\begin{aligned}\hat{X}'(z)&=\hat{D}'(z)\cdot G^{-1}+\sum_{k=1}^{P}\alpha k\cdot\hat{X}'(z)\cdot z^{-k}\\&=\hat{D}'(z)\cdot G^{-1}+P(z)\cdot\hat{X}'(z)\ .\end{aligned} \qquad --(27)$$

Thus

$$\hat{X}'(z)=\frac{G^{-1}\cdot\hat{D}'(z)}{1-P(z)}\ .$$

	Level A	Level B	Level C
Sampling frequency (KHz)	37.8	37.8	18.9
Residual word length (bits per sample)	8	4	4
Number of samples per sound block	28	28	28
Range data (bits per sound block)	4	4	4
Range values	0-8	0-12	0-12
Filter data (bits per sound block)	1	2	2
Number of filters used	2	3	4
Average of bits used per sample (bits per sample)	8.18 =(8x28+4+1)/28	4.21 =(4x28+4+1)/28	4.21 =(4x28+4+1)/28
Channel bit rate (Kbits per second)	309	159	80

Table I. The parameters for each level

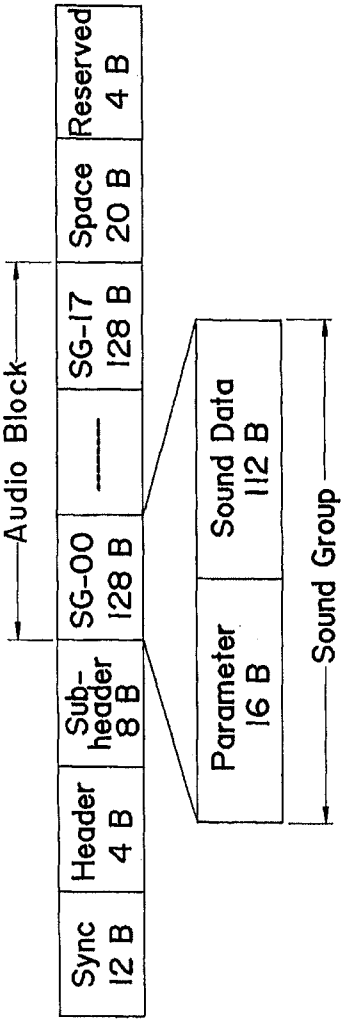

Figure 1. Data structure of the CD-I audio sector

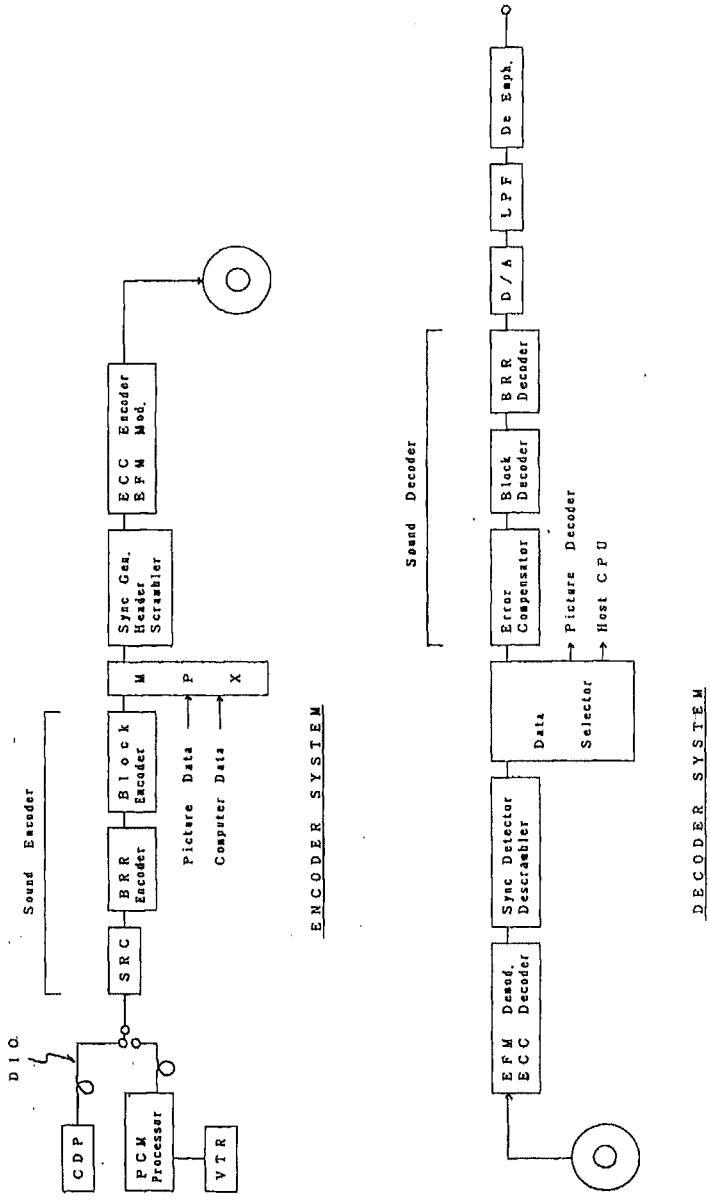

Figure 2. Block diagram of the prototype CD-I encoder/decoder system

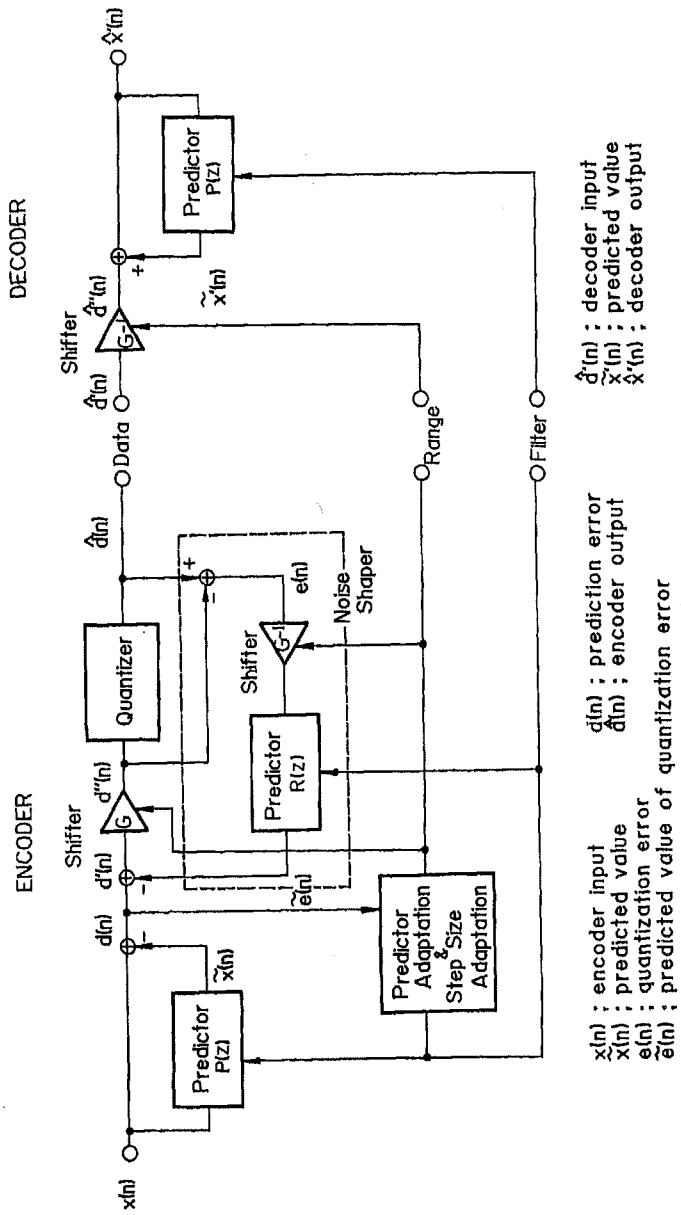

Figure 3. Block diagram of the Bit Rate Reduction System

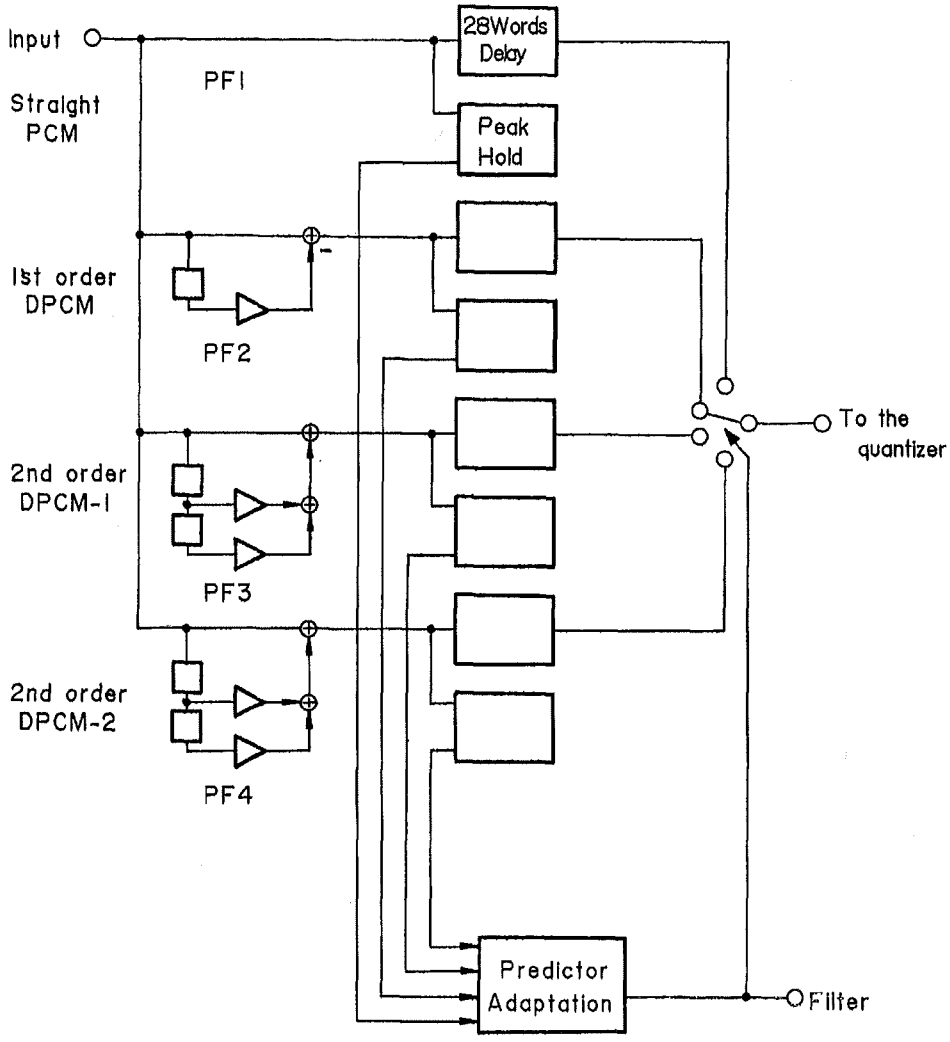

Figure 4. Detailed configuration of the prediction filters

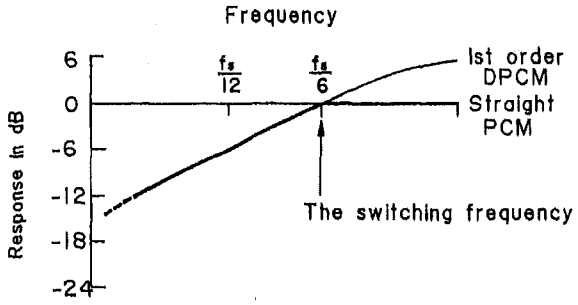

Figure 5. Switching frequency between 1st-order DPCM and straight PCM. The heavy line designates the system response.

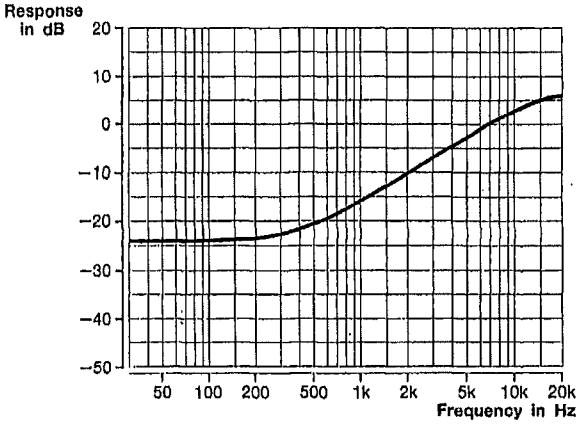

Figure 6. Frequency response of prediction filter 1st-order DPCM ; $H(z)=1-0.9375 \cdot z^{-1}$ when fs=37.8 KHz

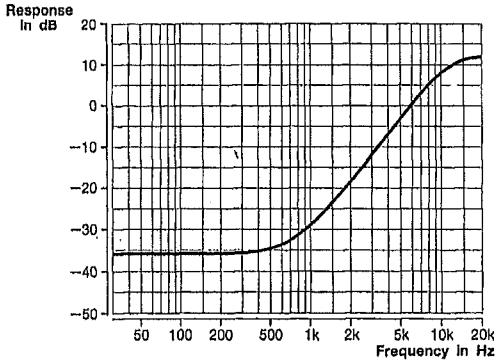

Figure 7. Frequency response of prediction filter
2nd-order DPCM-1 : $H(z)=1-1.796875\cdot z^{-1}+0.8125\cdot z^{-2}$
when fs=37.8 KHz

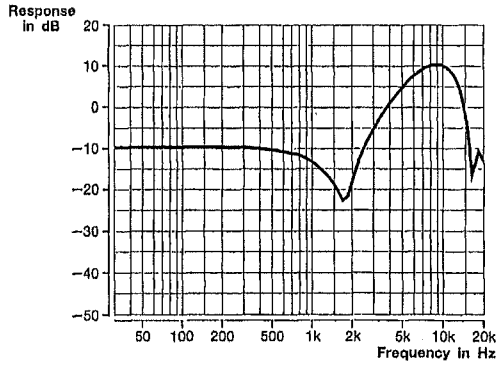

Figure 8. Frequency response of prediction filter
2nd-order DPCM-2 : $H(z)=1-1.53125\cdot z^{-1}+0.859375\cdot z^{-2}$
when fs=18.9 KHz

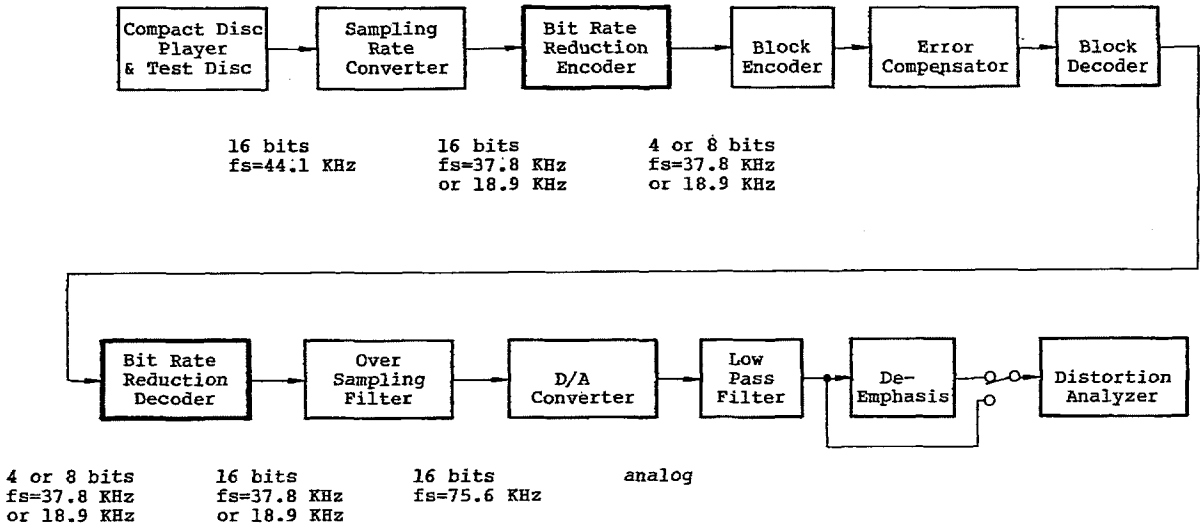

Figure 9. SNR measurement block diagram

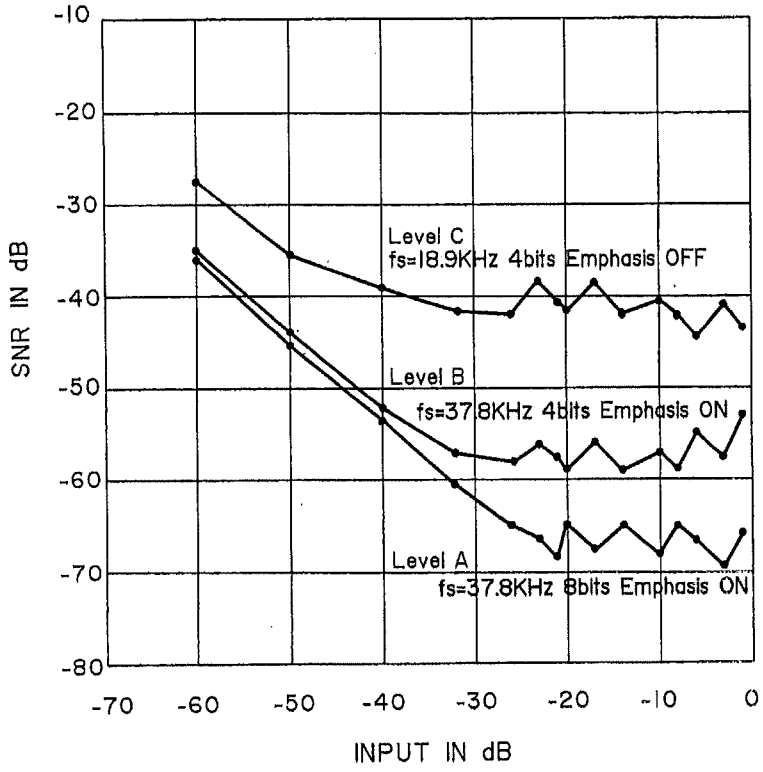

Figure 10. Signal-to-noise ratio versus input at each level
Input : 1-KHz sine wave

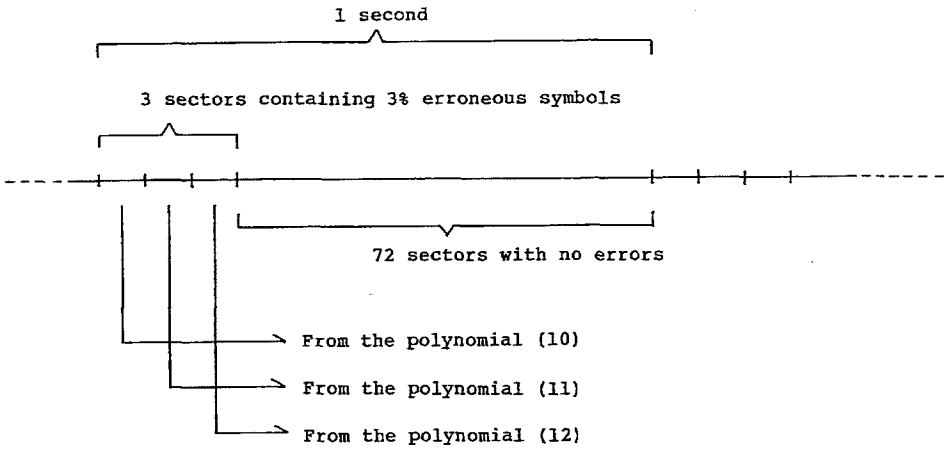

Figure 11. Distribution of the simulated code errors

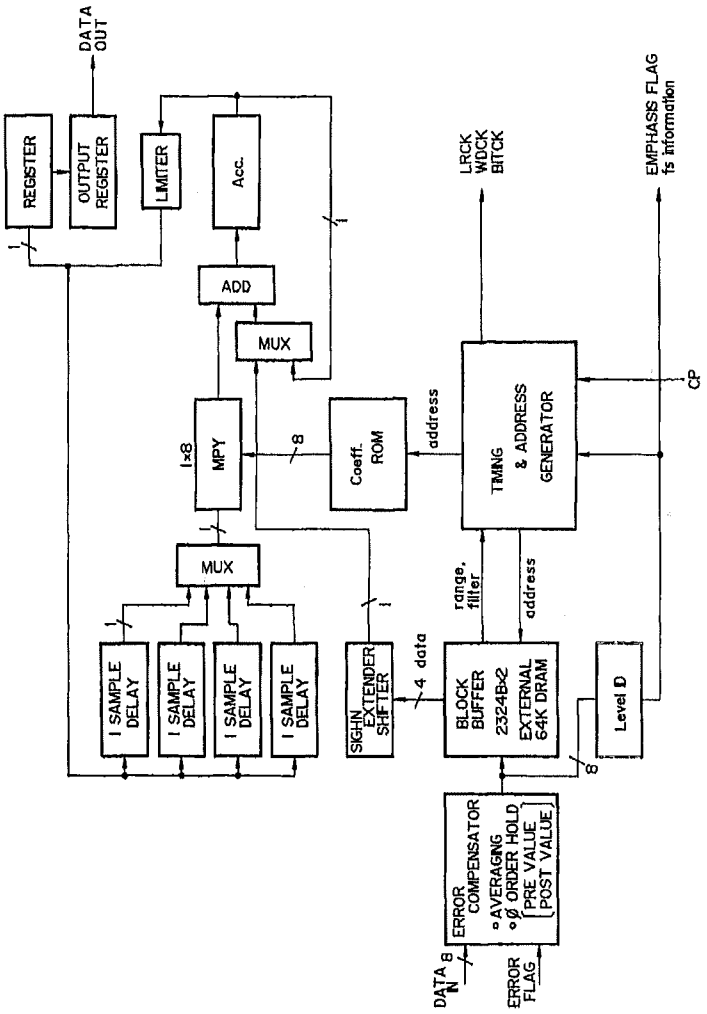
DATA OUT
REGISTER
OUTPUT REGISTER
LIMITER
Acc.
ADD
MUX
MPY
I×8
8
Coeff. ROM
address
TIMING & ADDRESS GENERATOR
LRCK WDCK BITCK
EMPHASIS FLAG fs information
CP
MUX
I SAMPLE DELAY
I SAMPLE DELAY
I SAMPLE DELAY
I SAMPLE DELAY
SIGN EXTENDER SHIFTER
4 data
range, filter
address
BLOCK BUFFER 2324B×2 EXTERNAL 64K DRAM
Level D
ERROR COMPENSATOR
∘ AVERAGING
∘ Ø ORDER HOLD
PRE VALUE
POST VALUE
DATA IN
ERROR FLAG

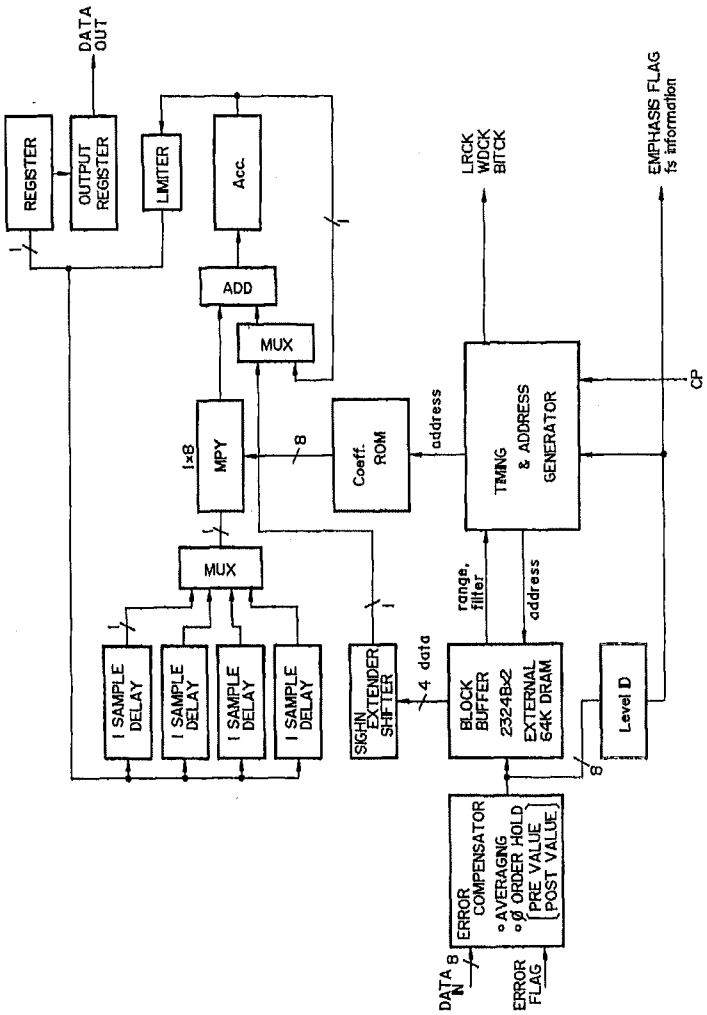

Figure 12. Block diagram of the CD-I Audio Processor LSI